Detuning of Pelton Runners

Joachim Schmied
DELTA JS Ltd.
Technoparkstrasse 1
CH-8005 Zurich
jschmied@delta-js.ch

Thomas Weiss
VA TECH HYDRO Ltd.
R&D Department
Hardstr. 319
CH-8023 Zurich
thomas.weiss@vatech-hydro.ch

Richard Angehrn
VA TECH HYDRO Ltd.
R&D Department
Hardstr. 319
CH-8023 Zurich
richard.angehrn@vatech-hydro.ch

ABSTRACT

The goal of the presented detuning procedure is to prevent resonances of Pelton runners in water turbines. The buckets of these runners are dynamically excited by the impact like jet load of the fluid. Primarily in multi-jet turbines, the resonance peaks can increase beyond detrimental limits of dynamic stress, causing high cycle fatigue and risk of cracking.

Detuning, if necessary, is practically executed by grinding a bucket very specifically and locally on its backside. Since the stiffness is much less affected by this action than the mass the concerned natural frequency of the bucket is tending to increase. Mass corrections in the range of some kilograms per bucket (some percent of the bucket's mass) normally are sufficient to move outside of the forbidden frequency band. They also do not harm the structural integrity of the runner.

In the paper it is shown how a mathematical model of the runner can be obtained from a vibration measurement executed on the finished runner. The model allows in a first step to check if corrections are necessary, and, if yes, in further steps to simulate modifications and find optimal mass corrections of the buckets with regard to the natural frequencies and the runner's unbalance, caused by these corrections. A possible de-balancing of the runner has to be compensated by removing material from appropriate locations of the runner.

KEY WORDS

Pelton runner safety, avoidance of resonance, avoidance of high cycle fatigue, mathematical model simulation, prediction of optimal corrections

1 INTRODUCTION

Most of the worldwide installed runners are still mono-block cast stainless steel runners where the buckets' mass can vary due to the not fully machined bucket backside. This, in combination with a coupling between the buckets through the wheel disk, gives rise to a complex vibration system. Therefore, a precise prediction of the natural frequencies by using the Finite Element Method (FEM) on a model, gained from design data, is not reliable enough. Newer technologies with welded, forged and milled fabrication (e.g. MicroGuss or HIWELD) reduce the mass scatter by complete machining of the runner and allow better vibration predictions by FEM.

The actual dynamic system, consisting of a number of slightly different buckets coupled by the runner disk, is complex and different from the theoretically, by FEM, investigated system. In the past, each bucket was regarded as a single-degree-of-freedom system, separated from the others. Corrections of the natural frequencies, if necessary, were executed by grinding the rear of the concerned buckets. Subsequent checks, however, sometimes revealed unexpected deviations. The reason is that the system cannot be separated as described above. It must be regarded and analysed as a multi-degree-of-freedom system. Therefore, a new detuning procedure was to be developed. The aim was to optimise and accelerate the process of final bucket grinding. Not only should the natural frequencies be regarded but also the final runner balancing which has to meet the quality requirements of ISO 1940-1 [11].
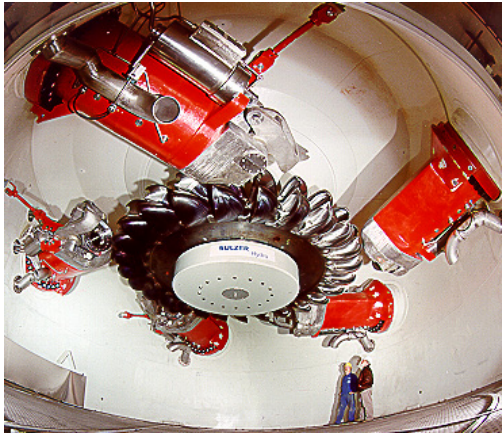
Figure 1 gives an insight into one of the turbine chambers of the world's most powerful Pelton turbines at *Bieudron*[1] in Switzerland, where the runner with the buckets can be recognized, surrounded by the 5 injectors.

Some characteristic data of the *Bieudron* Pelton turbines are shown in the Tables 1 and 2. Further references on this record breaking project are [1], [2], [3], [4].

Figure 1: Insight into one of the *Bieudron* turbines.

Table 1: Turbine data

Number of turbines		3
Rated plant output		1200 MW
Rated turbine output	P	423 MW
Rated head H		1869 m
Synchronous speed	n	428.57 min^{-1}
Runaway speed		756 min^{-1}
Rated flow		25 m^3/s
Jet pitch diameter		3993 mm
Number of nozzles	Z_0	5

Table 2: Runner data

Outer diameter	4630 mm
Width of buckets	620 mm
Number of buckets	26
Weight of runner	29000 kg
Weight of a bucket	380 kg
Max. jet force	944 kN
Centrifugal bucket force at synchronous speed	1470 kN
Type of coupling	Friction type
Material / stainless cast steel	G-X5 CrNi 13 4

2   HYDRAULIC EXCITATION

$\Delta\sigma_B$ = superimposed dynamic stress part due to harmonic response

$\Delta\sigma_J$ = dynamic stress part due to jets

σ_c = centrifugal stress

σ_a = stress amplitude
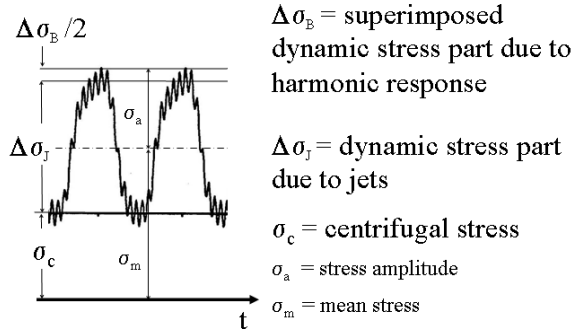
σ_m = mean stress

Figure 2: Measured stress trace of a bucket at its root.

A typical stress trace for locations at the bucket root, in the fillet of the middle ridge is given in figure 2. It is measured on a 6-jet prototype runner at normal operation and contains two jet impingements. Two dynamic stress parts can be recognized: The one consisting of the lower frequency part due to the jets ($\Delta\sigma_J$) and the other as superimposed higher frequency part due to the harmonic bucket response ($\Delta\sigma_B$). The better the coincidence of the exciting frequencies with natural frequencies of the buckets the more pronounced is the superimposed stress.

In general, fatigue by $\Delta\sigma_J$ is the primary cause of damages [5], [6], [7]. The calculation of $\Delta\sigma_J$ can be done reliably and measures against too high $\Delta\sigma_J$ can be taken by design improvements, reducing stress concentrations and by respecting adequate safety factors. The prediction of $\Delta\sigma_B$ is much more difficult and adequate measures to limit $\Delta\sigma_B$ are a challenge. Although there is a problem to differentiate between the two sources of fatigue damages, in practice cases are known, where a suspicion for resonance arose and where $\Delta\sigma_B$ was probably too high and initiated the crack. Resonance can increase the superimposed stress $\Delta\sigma_B$ drastically due to the low damping and the dynamic magnification factor which can grow up to 1000. This urges the designer of multi-jet runners to take into account also harmonics of increased order number i = 12 to 16 or even higher.

---

[1] The power station *Bieudron* was successfully commissioned by the end of 1998. During the first two years of operation the 3 units operated between 2644 and 3425 hours and the runner buckets experienced up to 350 million load cycles by jet impingement. On December 12, 2000, the *Cleuson-Dixence* penstock collapsed on an axial length of 9 meter and 3 people died due to the accident. Since then all machines are down. The rehabilitation of the penstock is now going ahead and the recommissioning of the plant is scheduled for 2009.

The goal of the defined detuning project was to get the know how for a procedure, which avoids resonances by preventing a coincidence of the natural frequencies of the bucket bending vibrations (figures 6 and 7) with multiples of the basic excitation frequency f_1.

Assuming that the bending moment characteristic of figure 3, determined by strain gage measurement on a scaled down model runner, is transferable to the full size prototype and allows to derive the jet impingement force, the discrete Fourier spectrum of the bucket excitation force can be established (figure 5).
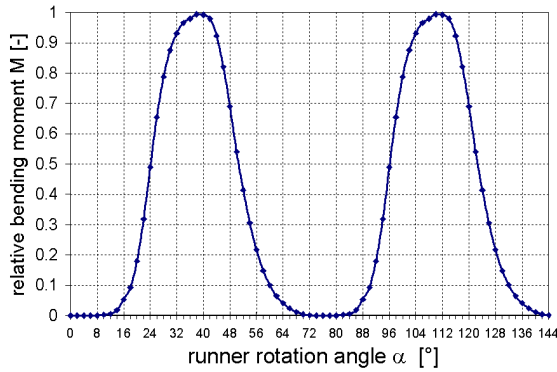
Figure 3: Characteristic of the bending moment at the bucket root over two jet impingements.
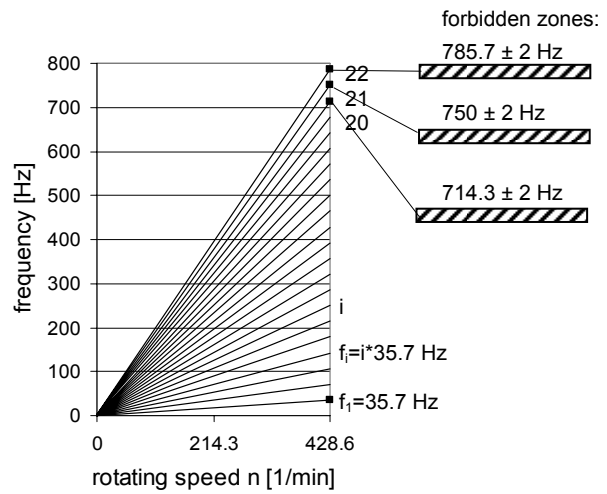
Figure 4: Campbell-diagram of the excitation due to the jet pulsation and definition of forbidden frequency zones.

The Campbell-diagram in figure 4 shows the excitation frequencies over variable rotating speed up to nominal speed n=428.6 rpm. The basic frequency f_1 = 35.7 Hz is the frequency of each bucket passing the 5 evenly distributed jets. The harmonics i = 20 to 22 may collide with natural frequencies (figure 7). That's why forbidden zones of ±2 Hz had been defined which would avoid a magnification > 200. Lower harmonics can collide with frequencies of vibration modes with zero or one nodal diameter. However, these modes cannot be excited by the five nozzles and are therefore not further considered.

Impingements by the jets, as shown in figure 3, are running in 3 phases: The jet stream starts striking the empty bucket and increases its loading (1). The full stream of the jet is loading the bucket with about double speed of the bucket (2). The jet stream is decreasing and the loading ends when the bucket is empty (3). The exact curve may vary slightly, depending on the hydraulic profile of the buckets which influences the Fourier spectrum of figure 5, especially the higher harmonics.
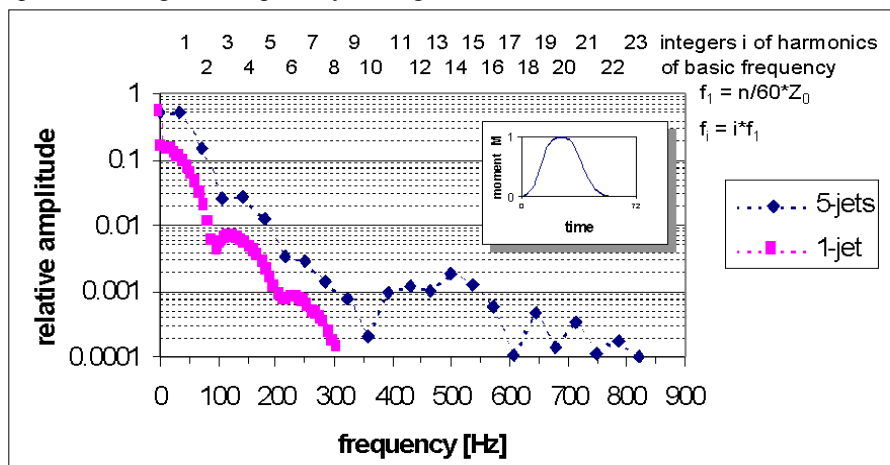
Figure 5: Discrete Fourier spectrum of the jet impingement force on the prototype *Bieudron* for the 1- and 5-jet operation (Z_0 = 1 and 5). The frequency steps for 1 and 5-jet operation are 7.14 Hz and 35.72 Hz, respectively.

Figure 5 lets us recognise that the amplitudes at 1-jet operation are 5 times smaller compared with 5-jet operation and with 6 jets it would be 6 times. Amplitudes < 1E-4 are regarded as uncritical whereas those > 1E-3 are regarded as critical. Due to the high magnification up to 1000 the bucket could then respond with a stress amplitude higher than $\Delta\sigma_J$. Amplitudes in the range between 1E-4 and 1E-3 are of medium importance. However, to be sure, they had been taken into account at the *Bieudron* project.

3 NATURAL FREQUENCY BEHAVIOUR

Figure 6: Typical natural modes of a Pelton bucket.
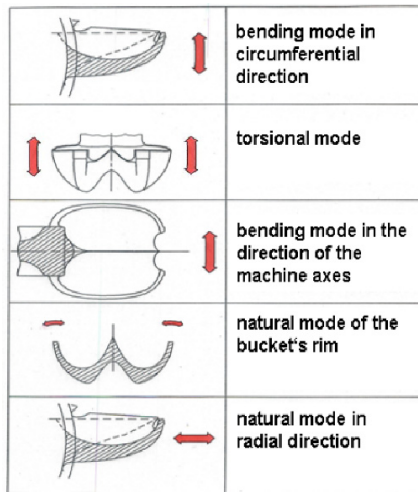
Some typical natural bucket modes are shown in figure 6. The relevant mode in operation is the bending mode in circumferential direction, which, in some cases, can be combined with a vibration of the buckets's rim.

The theoretical modal analysis by FEM assumes identical mass and stiffness of all buckets and is an idealisation. The reality can be different, since with integrally cast runners the buckets are not fully machined at the rear; their geometry can deviate from the precise design profile. This causes some scatter of the bucket geometries.

The lowest six natural modes of the model are shown in figure 7. It can be seen, that for the natural modes with a higher number of nodal diameters, the mode shape resembles a pure bucket vibration. The frequencies of these modes are almost equal. In case of the theoretical model with identical buckets the 5 jets would excite the 6th mode with 5 nodal diameters at 762Hz, the lower modes shown in the figure would not be excitable.

Measurements by hammer excitation at the bucket centre normally show the frequencies of bucket modes, i.e. of the modes with participation of mainly the bucket. However, these frequencies have a considerable scatter due to the mentioned deviations between the buckets.

A frequently asked question concerns the added mass influence of the water. This was investigated and answered during the course of earlier measurements [5]. It was found that the added mass effect, lowering the natural frequencies, was compensated by the stiffening effect due to the centrifugal forces. Moreover both effects are small, the centrifugal effect due to the low speed and the high bucket stiffness, the added mass effect due to the soft coupling of the water mass with the bucket. Therefore, they are neglected here.
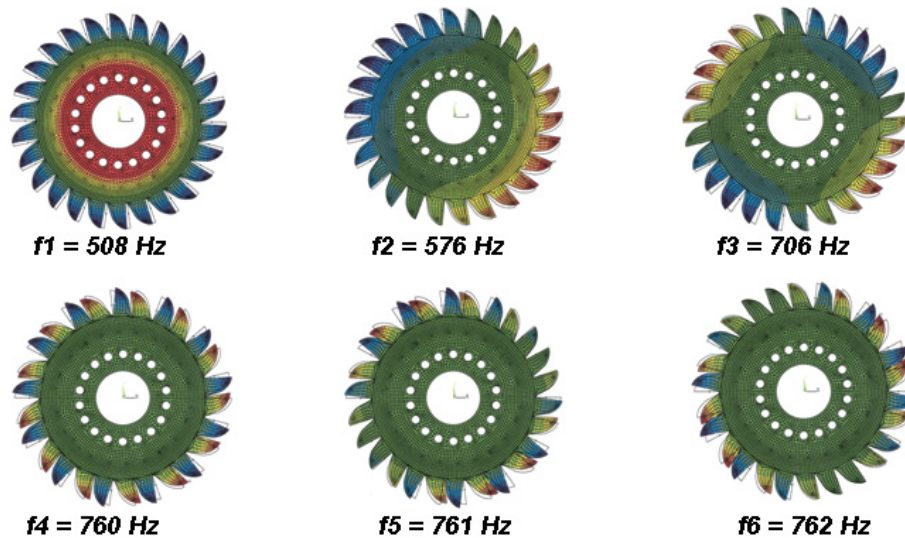

Figure 7: Calculated frequencies of the lowest 6 natural modes of bucket bending vibration: f^i (i=1-6) = 508 / 576 / 706 / 760 / 761 / 762 Hz (i = number of mode, n = i–1 = number of nodal diameters).

4 SIMPLIFIED MODELS: SINGLE-MASS AND COUPLED MULTI-MASS SYSTEM

The modes of the runner with a higher number of nodal diameters as well as the modes excitable by hammer excitation at the buckets have the character of a single bucket vibration. As a first simple approach it is therefore obvious to consider the bucket as a single-mass system, which is also used to define a forbidden frequency zone for the natural frequencies.

The amplification function of a single-mass system is shown in figure 8. It shows the response amplitude as a function of the excitation frequency. The frequency is relative to the natural frequency, and the response force amplitude at the root is relative to the excitation force amplitude. Stress analyses on the basis of the measured excitation spectrum shown in figure 5 proved, that an amplification of 200 should not be exceeded, which defines the forbidden frequency zone as shown in figure 8.
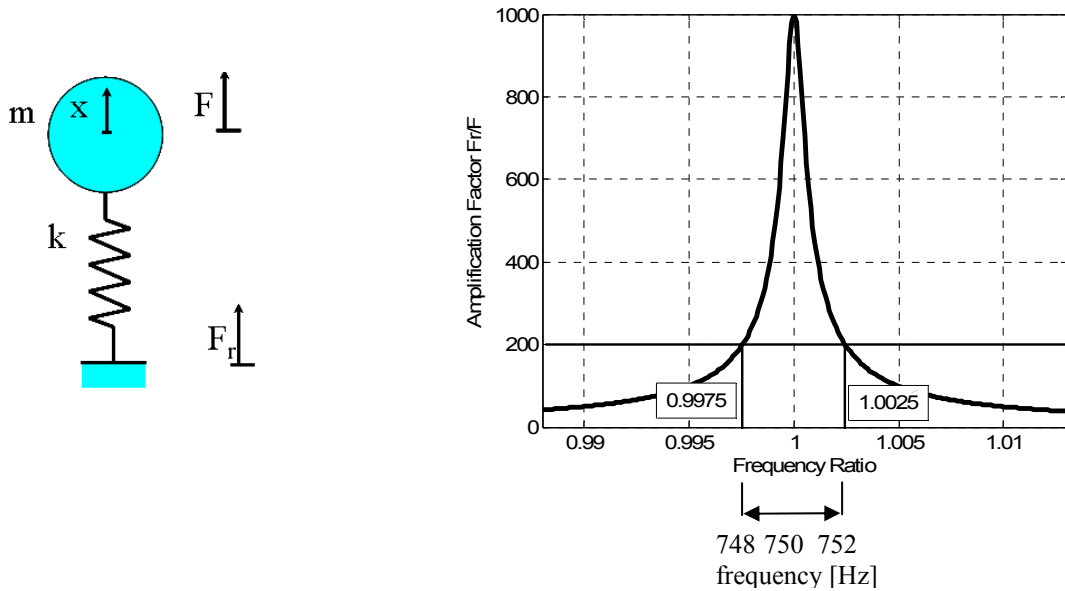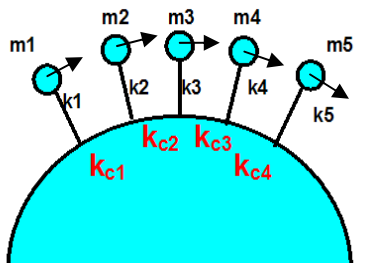
Figure 8: Amplification factor of a one-mass system and forbidden frequency zone, damping ratio 0.5‰.

Due to the geometry scatter of the buckets and also due to the coupling of the buckets via the disk a coupled multi-mass system as shown in figure 9 is more realistic. In this model the mass and the stiffness representing the bucket as well as the coupling stiffness may be different for each bucket. The parameters of this model are identified from a measurement of the runner.

Figure 9: Coupled multi-mass system as model of a Pelton runner.

5   IDENTIFICATION OF THE PARAMETERS OF THE COUPLED MULTI-MASS SYSTEM
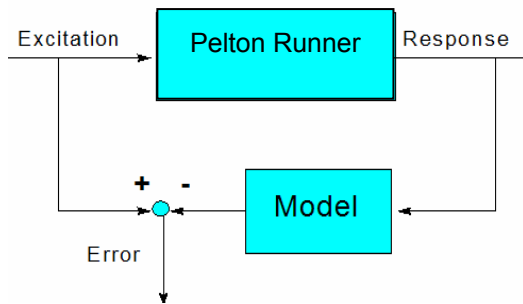
The principle of the identification as shown in figure 10 can be described as follows: The runner is excited at each bucket. From the response of each bucket the excitation is estimated by means of a model. The estimated excitation is compared with the actual excitation. The model is determined by minimising the error between the two excitations.

Figure 10: Principle of the identification.

The basic equation of the method is (see [9]):

$$\boldsymbol{H(\omega)\ S(\omega) = E + R(\omega)} \tag{1}$$

with $\boldsymbol{H(\omega)}$ as the matrix of dynamic flexibilities (= measured transfer functions),
   $\boldsymbol{S(\omega)}$ as the matrix of dynamic stiffnesses of the model,
   $\boldsymbol{E}$ as the unit matrix, corresponding to the excitation if the transfer function is regarded as response,
   $\boldsymbol{R(\omega)}$ as the residual matrix corresponding to the error of the estimated response,
   ω as the frequency.

The matrix $\boldsymbol{H}$ contains the measured transfer functions $h_{ik}(\omega)$ as indicated in (2), i.e. the response at a coordinate i to an excitation at the coordinate k. Each bucket is represented by a coordinate in circumferential direction. The matrix $\boldsymbol{H}$ must contain all transfer functions $h_{ik}(\omega)$, which means that it is a square matrix with a dimension corresponding to the number of buckets. Since the matrix is symmetric, either the full upper or lower triangle of the matrix must be measured as described in the next chapter.

Paper-ID 112.00

$$H = \begin{bmatrix} h(\omega)_{11} & & & symmetric \\ h(\omega)_{21} & h(\omega)_{22} & & \\ h(\omega)_{31} & h(\omega)_{32} & h(\omega)_{33} & \\ \vdots & \vdots & \vdots & \ddots \end{bmatrix} \tag{2}$$

The matrix of dynamic stiffnesses can be calculated as follows from the structure matrices of the model:

$$S(\omega) = -M \, \omega^2 + j \, \omega D + K \tag{3}$$

with M as the model mass matrix of dimension n x n,
$\quad$ D as the model damping matrix of dimension n x n,
$\quad$ K as the model stiffness matrix of dimension n x n,
$\quad$ n as the number of buckets (= number of coordinates of the model).

In case the model would be able to exactly reproduce the measured transfer functions by inversion of S, the residual matrix R in (1) would be a zero matrix. Due to the simplifications in the model and due to inaccuracies of the measurement this will never be the case. Therefore the aim is to minimise R.

The solution of equation (1) for the unknown matrices M, D, K requires a sufficient number of equations. For one frequency there are 2 matrix equations of the dimension n x n to solve the three unknown matrices of dimension n x n. The two matrix equations correspond to the real and imaginary part of (1). This means that one frequency is not sufficient to solve all unknowns. In practice many frequencies are used. It is obvious to solve the over-determined equation (1) by a least square fit of R, which means to solve the equation

$$A^T A \, X = A^T B \tag{4}$$

where A contains the real and imaginary parts of the dynamic flexibilities for different frequencies,
$\quad$ B contains unit matrices for the real parts and zero matrices for the imaginary parts and
$\quad$ X contains the unknown structure matrices in the form

$$X^T = (K^T, M^T, D^T) \tag{5}$$

Equation (4) is gained by rearrangement of (1) after substituting (3) into (1).

However, in case of measured transfer functions with some noise content, this method does not yield good results. This is due to the reason, that the unknown are coupled with the noisy transfer functions by multiplication. Therefore in [10] a method is proposed, which is based on the introduction of an instrumental variables matrix. Instead of equation (4) the following equation then is solved:

$$W^T A \, X = W^T B \tag{6}$$

with W as the matrix of instrumental variables.

W also contains dynamic flexibilities, however not the measured flexibilities, which are only used in a first step. In this first step the method is identical to a least square fit, i.e. to a solution of equation (4). In subsequent steps dynamic flexibilities are calculated from the identified structure matrices and used as W in equation (6), which is solved again. Hence the method consists of the following steps, which considerably reduces the influence of noise:
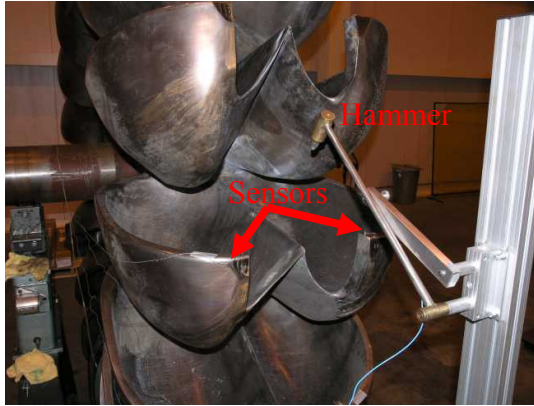
1. Setting up **A** and **W** from measured flexibilities.
2. Solution of (6), which is identical to (4).
3. Calculation of dynamic flexibilities from identified structure matrices.
4. Setting up **W** with the calculated dynamic flexibilities.
5. Solution of (6).
6. Repetition of steps 3 to 5 until sufficient convergence of the identified parameter is achieved.

The practical application of the method proved, that the quality of the results (convergence, physical plausibility) improved considerably when reducing the number of unknown parameters. The following measures were taken to achieve this:

- The mass matrix was assumed as diagonal.
- For the stiffness matrix only a limited number of buckets were coupled, which limited its bandwidth.
- The damping matrix was assumed as proportional to the stiffness matrix. The proportionality factor was chosen to yield a damping factor in the frequency range of interest of D = 0.05%. This damping factor could well be determined from resonance peaks.

6 MEASUREMENT AND EVALUATION

The full lower triangle of the dynamic flexibility matrix in equation (2) is measured by hammer excitation of each bucket. The measurement procedure was optimised to reduce the measuring time and to obtain the required accuracy. Figure 11 shows the measurement set up. A special pendulum for the hammer excitation was developed in order to achieve a clear excitation in circumferential direction at the outer diameter of the bucket's middle ridge. Very light accelerometers are applied at the rim on both sides of a bucket. The signals of the two sensors are averaged to eliminate any influence of the bucket torsional mode. Several buckets are equipped with pairs of sensors in one set up thus measuring their response to a hammer excitation simultaneously. The number of buckets per set up depends on the number of channels of the data acquisition system. In order to receive the full triangle of the dynamic flexibility matrix several set ups with excitations at different buckets are necessary: In the first set up only the buckets equipped with sensors are excited thus measuring the full sub-matrix corresponding to the equipped buckets. In the following set ups all buckets equipped with sensors plus those measured in the previous steps are excited thus also measuring the matrix coupling terms between the currently and previously equipped buckets.

Figure 11: Locations for the excitation (on the middle ridge) and the response measurement (on the bucket rim).

The measured direct transfer functions (excitation and response at the same bucket) of two buckets are shown in figure 12. The left as well as the right signal are shown. They coincide well. Important parameters of the measurement are:

- Frequency range: 608 to 1008 Hz
- Frequency step: 0.25 Hz

The frequency step must be chosen in accordance with the sharp resonance peaks, which have a half power width of less than 1Hz due to the low damping.

The transfer function h_{1919} has one dominating peak with a high maximum value, whereas h_{2525} has many peaks at a lower level. The vibration of bucket 25 is strongly coupled with other buckets. The maximum peaks of the off diagonal transfer functions, which are not shown here, generally have lower peaks.
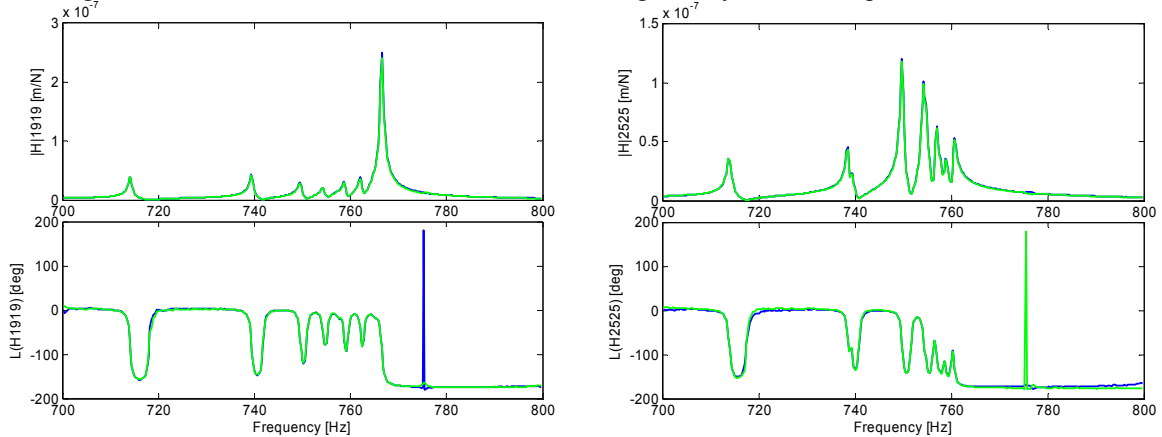

Figure 12: Direct transfer functions of the buckets 19 and 25 (left and right signal)

The identification of the model by means of the measured transfer functions is carried out with the following parameter:

- Damping ratio at 750 Hz: 0.05%, (yielding a proportionality factor for the stiffness of β=2.12 10^{-7} s)
- Number of coupled buckets: 7
- Frequency range: 752Hz to 770Hz

The direct transfer functions calculated from the identified model in comparison to the measured transfer functions are shown in figure 13 for the buckets 8,19,22,25. It can be seen that the model is able to represent the measured behaviour very well in the frequency range from 754Hz to 770Hz. At lower frequencies there is some deviation. As we will see, this is due to the disk character of the modes in this frequency range.
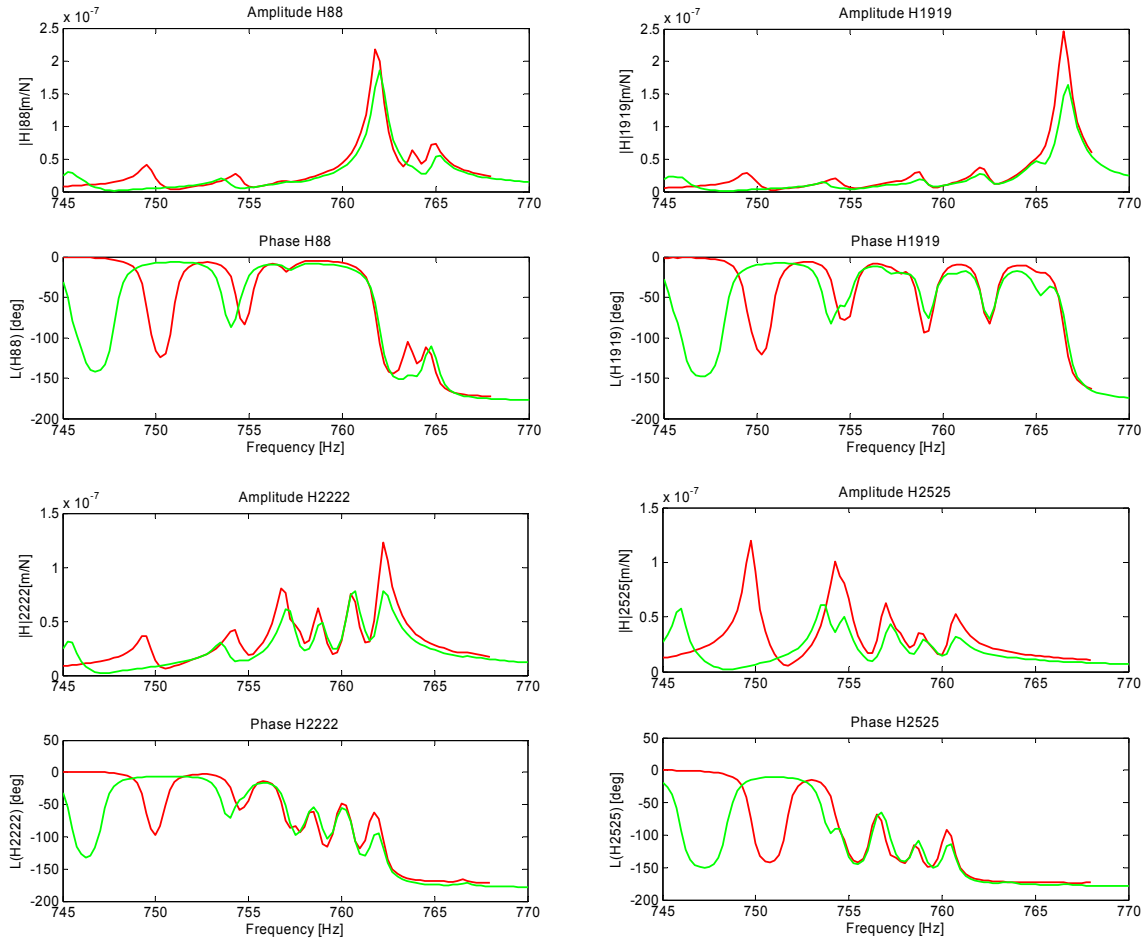
Paper-ID 112.00

Figure 13: Measured (red) and model based (green) direct transfer functions of the buckets 8, 19, 22 and 25.

The average mass and direct stiffness of the identified model are as follows:
- Average masses of the identified model: $m = 90.33\text{kg}$
- Average direct stiffness of the identified model: $k = 1.8525 \cdot 10^{9}$ N/m

Some natural modes of the identified model in the frequency range of interest are shown in figure 14. As mentioned above the modes in the lower frequency range have disk character, which can be recognised by the sine-shaped deflections of the masses around the circumference. In case of the modes in the higher frequency range fewer masses participate.
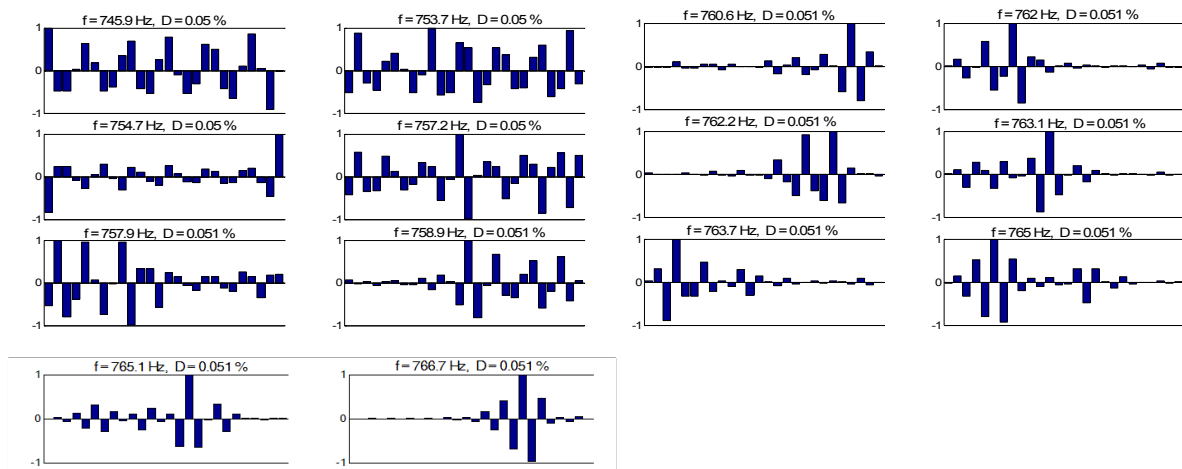

Figure 14: Natural modes of the identified model (x-axis: Bucket number; y-axis: Bucket bending displacement).

Paper-ID 112.00

The quality of the identified model is assessed by the following criteria:
- Convergence of the identification process, i.e. of the identified masses and stiffnesses.
- Physical plausibility of the identified masses and stiffnesses, e.g. a negative mass does not make sense.
- Comparison of the measured and model based transfer functions as in figure 13, by visual assessment.
- Physical plausibility of the eigenvalues of the identified model, mainly the damping ratio.

The assessment requires some experience and should only be done by qualified personnel. The quality can be influenced by the number of coupled buckets and to a high extent by the selected frequency range for the identification. Modes, which do not have the character of a bucket mode, i.e. the disk modes in the lower frequency range, should be eliminated as far as possible.

It should be noted that the method does not identify the parameter, e.g. the mass with such accuracy, that they represent the real mass scatter. However, the model is able to represent the vibration behaviour in the frequency range of interest and accurately predicts the influence of mass changes as we will see in the following chapter.

7 CORRECTION

The masses of buckets must be reduced in the following cases:
1. A resonance is in the forbidden frequency range according to figure 4 and the peak exceeds the allowable value according to an amplification of $AF=200$ (see figure 8).
2. The unbalance of the runner exceeds the allowable unbalance.

The allowable peak amplitude can be calculated from the mean static stiffness and the amplification factor by

$$h_{max} = \frac{AF}{k}, \qquad (7)$$

which yields a value of $h_{max} = 0.11$ μm/N.

In the present case the only bucket, which has the largest peak of its direct transfer function in the forbidden range is bucket 25 (see figures 12 and 13). The frequency is at 749.75Hz. It is in the forbidden range from 748Hz to 752Hz (see figure 4). The bucket is strongly coupled and its resonance peak of 12 μm/N is at the allowable limit. The resonance is in the range of disk modes, where the model already deviates to some extent from the measurement. The corresponding mode of the model has the frequency 745.9Hz.

Furthermore, the unbalance of the runner exceeded the allowable limit of G2.5. Since the only resonance in the forbidden frequency range is at the allowable limit, emphasis was put on the correction of the unbalance. The following correction was decided:
- Mass reduction of buckets 11, 12, 13, 14, 15 by 2kg.

The predicted natural modes most influenced by the reduction are shown in figure 15. The corresponding original modes in figure 14 are at 757.2Hz, 765.1Hz and 763.1Hz. After execution of the mass reduction another measurement was carried out and a new model was identified. The corresponding modes of figure 15 are shown in figure 16. It can be seen, that the prediction is excellent.
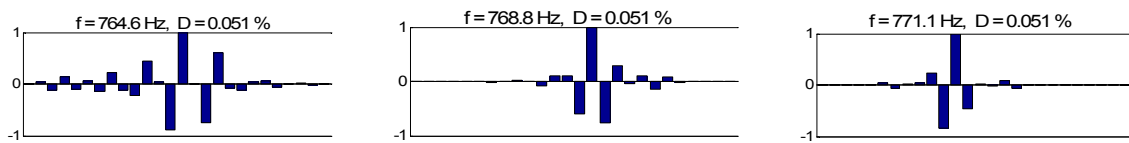

Figure 15: Predicted natural modes for the mass reduction (x-axis: Bucket number; y-axis: Bucket bending displacements).
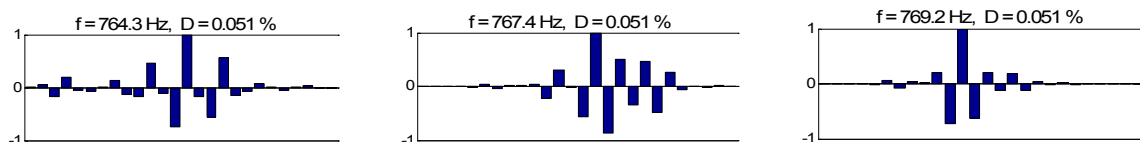

Figure 16: Natural modes from the model identified after the mass reduction (x-axis: Bucket number; y-axis: Bucket bending displacements).

The mode with the resonant bucket in the forbidden zone did not change its character and thus its excitability by the mass reduction. In the model the mass reduction increased its frequency from 745.9Hz to 747.1Hz. In the identified model after the mass reduction it has a frequency of 746.5Hz. In the measured transfer function of bucket 25 the resonant peak practically remained unchanged.

9   Paper-ID 112.00

8   SUMMARY

In order to prevent resonances of circumferential bucket bending modes with the impact like jet excitation detuning of the buckets can be necessary, and is practically carried out by mass reduction. The allowable unbalance must also be considered, when reducing the bucket masses. The Pelton runner has complex vibration behaviour, due to the scatter of the bucket geometries and due to the coupling of the buckets via the disk. To apply the correct mass reduction therefore is not an easy task.

A method based on the measurement of dynamic flexibilities of the buckets and the identification of a coupled multi-mass model is described, where each mass represents a bucket. The detuning can then be simulated with the model, before actually executing the mass reduction at the runner.

The identification yields a model, which is able to well describe the vibration behaviour in the frequency range of interest, especially if only a portion of the buckets participate. There are some deviations in cases where disk vibrations play a role. However, the latter are normally not of interest, since they are not well excitable.

In order to obtain useful models the number of model parameters has to be reduced as much as possible for the identification process. This is done by prescribing the damping, which is actually known, by assuming a diagonal mass matrix and a limited number of coupled buckets via the stiffness matrix, which limits its band width.

The method was developed for, and among others applied to the 29 tons Pelton runners of *Bieudron*, the hydropower station of *Cleuson-Dixence* in Switzerland, equipped with three turbines of 423MW power each. In the presented case a mass reduction was necessary to balance the runner. A coupled mode had an excitability at the allowable limit. The predicted behaviour for the proposed mass reduction coincided very well with the behaviour after its application. The method turned out to be an excellent aid for the detuning and balancing in many projects.

REFERENCES

[1]   Loth, P., "A record breaker. Cleuson-Dixence will go on line ...", Part "Hydromechanics", International Water Power & Dam Construction, June 1998, Pages 22-24.

[2]   Keck, H., Schärer, Ch., Cuénod, R., Cateni, A., "Pelton technology for new plants and modernization schemes", International journal on Hydropower & Dams, Vol. 4, Iss. 2, 1997, pages 104-108.

[3]   Bezinge, A., Bachmann, P., Vullioud, G., "Das Projekt Cleuson - Dixence", ÖVE/SEV/VDE/-Fachtagung "Wasserkraft - Regenerative Energie für heute und morgen", Vienna, May 1992.

[4]   Angehrn, R., "Safety Engineering for the 423 MW-Pelton-Runners at Bieudron", 20th IAHR Symposium August 6-9, 2000, Charlotte, N.C. USA

[5]   Angehrn R., Dubas M., "Experimental Stress Analysis on a 260 MW Pelton Runner", Proc. of the 11th IAHR-Symposium, Amsterdam, 1982.

[6]   Grein, H., Angehrn, R., Lorenz, M., Bezinge, A., "Inspection Periods of Pelton Runners", Proc. of the 12th IAHR-Symposium, Stirling, 1984.

[7]   Grein, H.L., Angehrn, R., "Service Life of Pelton Runners under Corrosion Fatigue", International Symposium on Fluid Machinery Troubleshooting, ASME Winter Annual Meeting, Anaheim, California, Dec. 1986, FED-Vol. 46/PWR-Vol.2.

[8]   Schmied, J., "Von der Schwingungsmessung zum Simulationsmodell", Technische Rundschau Nr. 17, Bern, 1998.

[9]   Schöllhorn, K., "Koordinatenreduktion durch Anpassung kinetischer Nachgiebigkeiten", Dissertation TH Darmstadt, 1984.

[10] Fritzen, Claus-Peter, "Identification of Mass, Damping and Stiffness Matrices of Mechanical Systems", Journal of Vibration, Acoustics, Stress and Reliability in Design, Vol 108, January 1986.

[11] ISO 1940-1:2003, "Mechanical vibration -- Balance quality requirements for rotors in a constant (rigid) state -- Part 1: Specification and verification of balance tolerances", 2003.